# Multi-scaled polymersomes from self-assembly of octadecanol-modified dextrans

Wen-Hsuan Chiang [a], Yu-Jen Lan [b], Yun-Chiao Huang [b], Yu-Wen Chen [b], Yi-Fong Huang [b], Sung-Chyr Lin [b], Chorng-Shyan Chern [c], Hsin-Cheng Chiu [a],*

[a] Department of Biomedical Engineering and Environmental Sciences, National Tsing Hua University, Hsinchu 300, Taiwan
[b] Department of Chemical Engineering, National Chung Hsing University, Taichung 402, Taiwan
[c] Department of Chemical Engineering, National Taiwan University of Science and Technology, Taipei 106, Taiwan

## ABSTRACT

Lipid-conjugated polysaccharide vesicles in nano- and micro-scale were developed from amphiphilic octadecanol-modified dextrans (OMD) prepared by partial esterification of dextran with activated octadecanol-carbamate imidazole in a well-controlled manner. The critical aggregation concentration (CAC) of OMD adducts in aqueous phase varies, depending mainly on their octadecanol contents. Through supramolecular assembly of the OMD adducts comprising either 17 or 28 mol% octadecanol residues with respect to the anhydroglucopyranose units by the partial solvent displacement technique with the initial water content of DMSO/H$_2$O solutions beyond a critical point, stable nano-scaled OMD assemblies were developed and characterized by the vesicle-like morphology. The dimension of polymersomes can be effectively controlled by the OMD composition as well as the initial water content. On the other hand, micro-scaled OMD polymersomes can be achieved by the double emulsion technique in a water/oil/water (w$_1$/o/w$_2$) manner. Both the contents of NaCl in aqueous solution as the w$_1$ phase and of DMSO in DMSO/CHCl$_3$ co-solvents as the organic phase, in which OMD was dissolved, are of great importance in controlling the polymersome morphology and size. These micro-scaled OMD polymersome walls are characterized by size-selective permeability capable of encapsulating large water-soluble cargoes while allowing transport of small polar species across the membrane, thereby rendering these unique colloidal particles of potential applications in biomedical technologies.

© 2012 Elsevier Ltd. All rights reserved.

## 1. Introduction

In the past decades, versatile polymer vesicles (also referred to as polymersomes) developed from self-association of various amphiphilic copolymers have attracted considerable interest owing to their potential applications in drug delivery, bio-diagnosis and catalysis [1–16]. To fulfill the requirement for the application of polymeric drug delivery vehicles in biomedical fields, biocompatible and biodegradable amphiphilic copolymers are promising candidates to serve as the major components of polymersomes. For example, vesicles attained from self-assembly of a biocompatible diblock copolypeptide, poly(L-glutamic acid)-b-poly(L-lysine), have been referred to as "schizophrenic" owing to the capability of undergoing reversible inversion of inner hydrophobic and outer hydrophilic regimes within vesicle walls in response to changes in medium pH between 3.0 and 11.0, while the copolymer retains an individual random coil conformation at neutral pH [11]. In addition,

as described by Armes and co-workers [12], when the solution pH was raised above 6.0, biocompatible diblock copolymer, poly(2-(methacryloyloxy)ethyl phosphorylcholine)-b-poly(2-(diisopropylamino)ethyl methacrylate) (PMPC-b-PDPA) underwent self-assembly into polymeric vesicles and an anticancer agent, doxorubicin (DOX), was concomitantly encapsulated in an efficient manner into the vesicle inner aqueous compartments. Structural dissociation of the assemblies at low pH via increased protonation of PDPA chain segments originally constituting hydrophobic layers implied the possibility of intracellular delivery of DOX. Rameez et al. successfully developed biocompatible and biodegradable polymersomes carrying hemoglobin for oxygen transport using diblock copolymers consisting of poly(ethylene oxide) as the hydrophilic block and either poly(ε-caprolactone) (PCL) or poly(L-lactide) as the hydrophobic block [14].

Owing to the unique characteristics such as excellent biocompatibility, biodegradability, nontoxicity, and protein-rejecting properties of polysaccharides [17–23], hydrophobically modified polysaccharides have also been widely used to prepare various types of polymeric assemblies, including micelles, vesicles and hollow capsules. Besheer et al. [17] prepared a series of

hydroxyethyl starch (HES) derivatives with different fatty acid contents via partial esterification. The modified polysaccharides thus obtained spontaneously associated into nano-scaled polymeric micelles and vesicles in aqueous phases. As reported by Liu and co-workers [18], hollow polysaccharide nanocapsules were readily obtained from association of the chitosan simultaneously modified by carboxymethyl and hexanoyl groups in an aqueous environment for potential controlled release of the encapsulated DOX. In addition, Zhang et al. [19] investigated the effects of the PCL content of PCL/dextran adducts on the morphological transition of the corresponding assemblies from micelles to vesicles in aqueous phase. Schatz et al. prepared polymersomes featured with a sharp mono-modal size distribution from hydrophobically modified dextran with poly(γ-benzyl L-glutamate) (PBLG) via the slow addition of excessive water into the solution of dextran/PBLG adduct in DMSO, followed by removal of DMSO by dialysis against water [24]. Houga et al. also reported that vesicles with a rather narrow size distribution were developed by assembly of dextran/polystyrene conjugates with high polystyrene contents in DMSO-rich co-solvent system with THF as the minor component or the pure water system [25].

In this work, a series of octadecanol-modified dextrans (OMD) were prepared by partial esterification of dextran with carbonyldiimidazole (CDI) activated octadecanol derivative (octadecanol-carbamate imidazole (CI)) in a well-controlled fashion. Dextran was selected as the hydrophilic part of the amphiphilic targets due to its excellent biocompatibility, aqueous solubility and non-fouling properties [20–23,26,27]. Nano- and micro-sized polysaccharide vesicles were then prepared by supramolecular packing of OMD via the partial solvent displacement and the $w_1/o/w_2$ type double emulsion techniques, respectively. The formation mechanisms and characterization of these OMD-based polymersomes were explored by dynamic and static light scattering (DLS/SLS), ^{1}H-NMR, transmission electronic microscope (TEM) and laser scanning confocal microscope (LSCM).
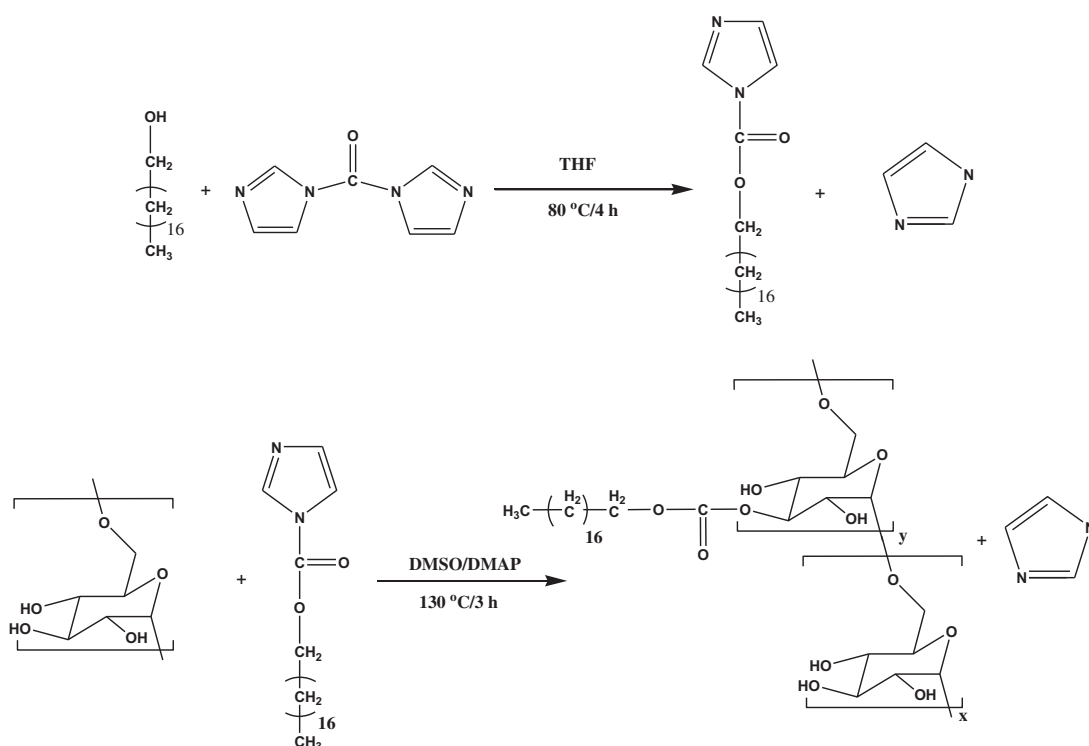
## 2. Experimental section

### 2.1. Materials

Carbonyldiimidazole (CDI), 1-octadecanol and 4-dimethylaminopyridine (DMAP) were purchased from Acros. Dextran T70 ($M_w$ ca 70,000 g/mol) was obtained from GE Pharmacia Biotech. Nile red and two fluorescein isothiocynate-dextrans (FITC-dextrans) ($M_n$ = 4 K and 10 K g/mol) were purchased from Sigma. Deuterium solvents used in ^{1}H-NMR measurements were obtained from Cambridge Isotope. Deionized (DI) water was produced from Milli-Q Synthesis (18 MΩ, Millipore). All other chemicals were reagent grade and used as received.

### 2.2. Syntheses of octadecanol-carbamate imidazole (octadecanol-CI) and OMD

Similar to the synthesis pathway for CDI-activated 2-hydroxyethyl methacrylate [28], Scheme 1 illustrates the method used to prepare octadecanol-CI in this work. In brief, CDI (15 mmol) was dissolved in anhydrous THF (20 mL), followed by the addition of 1-octadecanol (10 mmol). The reaction was carried out at 80 °C for 4 h under reflux. THF was then evaporated. The crude product was dissolved in chloroform and extracted with water to remove the by-product imidazole and unreacted CDI. The organic phase was collected and dried by anhydrous MgSO4. After removal of MgSO4 by filtration, octadecanol-CI was obtained by evaporation of chloroform under vacuum. The activation efficiency of 1-octadecanol by CDI was determined by ^{1}H-NMR using CDCl3 as the solvent.

The synthesis of OMD is described below (Scheme 1). Dextran T70 was dissolved in anhydrous DMSO and octadecanol-CI (10, 20, 30 or 40 mol% with respect to anhydroglucopyranose residues of dextran) was added into the reaction medium. The reaction was carried out at 130 °C for 3 h in the presence of DMAP as the catalyst.



**Scheme 1.** Synthetic route of octadecanol-modified dextrans (OMD).

The reaction solution was then subjected to dialysis (Cellu Sep MWCO 12,000–14,000) against DMSO/THF (2/1 (v/v)) to eliminate unreacted octadecanol-CI, followed by dialysis against DI water to remove DMSO and THF. The product was collected by lyophilization. The degree of substitution (DS) of dextran with 1-octadecanol defined hereinafter as the number of octadecanol group per 100 anhydroglucoside units was determined by $^1$H-NMR in DMSO-$d_6$ at 25 °C. FT-IR measurements of dextran, 1-octadecanol and OMD were conducted on a Perkin Elmer Paragon 500 using KBr tablet for the sample preparation. Four OMD products with varying DS values were prepared. The synthesis parameters, compositions, and conjugation efficiencies are summarized in Table 1. Each individual OMD is referred to hereinafter as a sample code (Table 1); for example, OMD9 represents the lipid-modified dextran adduct with a DS value of ca 9.

### 2.3. Determination of critical aggregation concentration (CAC)

The critical aggregation concentrations (CAC) of the resultant polysaccharide derivatives in aqueous phase were determined by the fluorescence technique using pyrene as a nonpolar probe [17,29,30]. The sample was dissolved in DMSO to different concentrations, followed by dialysis (Cellu Sep MWCO 6000–8000) against DI water for 2 days to remove DMSO. The final concentration of OMD in DI water was determined by lyophilization of the aqueous OMD solutions (suspensions) of prescribed volumes after dialysis. Aliquots (20.0 μL) of the pyrene solution ($3.0 \times 10^{-5}$ M) in acetone were evaporated in vials and then the above well stirred aqueous OMD solution (1.0 mL) was added. The resultant sample was mixed for 12 h, thereby leading to the solution with a constant pyrene concentration of ca $6.0 \times 10^{-7}$ M. Fluorescence characterization was carried out by determining the fluorescence intensity ratios ($I_3/I_1$) of the third vibronic band at 385.5 nm to the first at 373.5 nm of the fluorescence emission spectra of pyrene in aqueous solutions of OMD samples with various concentrations at 25 °C. The intensity ratio ($I_3/I_1$) represents a quantitative measure of the nonpolar nature of the microenvironment, in which pyrene resides. The higher the ratio, the more hydrophobic is the microenvironment. The excitation was performed at 336 nm and the emission was recorded in the range 350–500 nm on a Hitachi F-2500 fluorescence spectrometer.

### 2.4. Preparation of nano-scaled polysaccharide vesicles

OMD (2.0 mg) was dissolved in DMSO of a prescribed volume at 60 °C and, with the temperature being reduced to 25 °C, DI water was instantly added to reach a final OMD concentration of 2.0 mg/mL. The solution was under vigorous stirring for additional 20 min.

Polymersomes with nano-scaled size were obtained by dialysis of polysaccharide solutions (Cellu Sep MWCO 12,000–14,000) against DI water for 5 days to thoroughly remove DMSO.

### 2.5. Preparation of micro-scaled polysaccharide vesicles

Micro-scaled polysaccharide vesicles were prepared by a double emulsion technique in a $w_1/o/w_2$ form. OMD36 (4.0 mg) was first dissolved in the organic co-solvent (9.0 mL) comprising DMSO and CHCl$_3$ of differing volume ratios. An aqueous solution (4.5 mL) of NaCl at a preset concentration in the range 0.01–0.10 M as the internal aqueous phase ($w_1$) was mixed under vigorous stirring with the organic OMD solution by a homogenizer (Ika, T18) at 6000 rpm for 4 min. The $w_1/o$ emulsion thus obtained was rapidly added into DI water of 200 mL as the outer aqueous phase ($w_2$) under stirring at ambient temperature for 5 h to accomplish the $w_1/o/w_2$ emulsion and subsequent complete evaporation of CHCl$_3$. The polymersome suspension was further purified and concentrated by filtration using membrane filters (0.45 μm).

### 2.6. Dynamic and static light scattering (DLS/SLS) measurements

The mean hydrodynamic diameters ($D_h$) and particle size distributions of nano-scaled polymeric assemblies in DMSO/H$_2$O co-solvents and those in aqueous solutions resulting from thorough dialysis to remove DMSO were determined by a Malvern Zetasizer Nano-ZS instrument at a scattering angle of 173° equipped with a 4 mW He–Ne laser operating at $\lambda = 632.8$ nm, using the cumulant analysis method [31,32]. Prior to measurement, the OMD colloid was equilibrated at 25 °C for 30 min. The data reported herein represent an average of at least triplicate measurements.

For the purpose of assessing the morphology of polymeric assemblies in aqueous solutions, the ratio of the root-mean-square radius of gyration ($R_g$) to hydrodynamic radius ($R_h$) of particles was evaluated. The $R_h$ values were determined herein on a Brookhaven BI-200SM goniometer equipped with a BI-9000 AT digital correlator using a solid-state laser (35 mW, $\lambda = 637$ nm) at 90°. The CONTIN algorithm method was employed to analyze the DLS data in order to confirm the absence of bimodal particle size distribution of polymeric assemblies with much enhanced reliability [33,34]. In addition, the weight-average molecular weight and $R_g$ of polymeric assemblies were evaluated from the Berry treatment of the angular dependent measurements of the time-averaged intensity of scattered light for a series of concentrations of polymeric assemblies in aqueous suspensions [35,36]. The dn/dc values of the aqueous suspensions of polymeric assemblies were determined by a BI-DNDC differential refractometer ($\lambda = 620$ nm).

### 2.7. $^1$H-NMR measurements

First, the OMD sample was dissolved in DMSO-$d_6$ of a prescribed amount and the solution was stirred at 60 °C for 20 min. This was followed by the addition of D$_2$O at 20 °C until the target OMD concentration of 2.0 mg/mL was achieved. $^1$H-NMR measurements of polymeric assemblies in DMSO-$d_6$/D$_2$O solutions were performed on a Varian Unity Inova-600 at 600 MHz without sample spinning. The pulse width of 4.9 s with a relaxation delay of 2 s was utilized. Dry DMF in a sealed capillary coaxially placed in the NMR sample tube was repeatedly used as an external standard. The proton signal of DMF at 8.0 ppm was selected as the resonance reference for quantitatively determining changes in chemical shifts and signal intensities of feature signals of polymeric assemblies developed in DMSO-$d_6$/D$_2$O solutions with varying D$_2$O contents. Prior to measurements, the sample was equilibrated at 25 °C for 30 min.

**Table 1**
Synthesis parameters, compositions, average molecular weights and conjugation efficiencies of OMD adducts.

| Sample | Reaction feed (molar ratio) Glucopyranose/ octadecanol-CI | Composition ratio (molar ratio)[a] Glucopyranose/ octadecanol | Yield (wt%) | $M_w$[c] ($\times 10^{-4}$) (g/mol) |
|---|---|---|---|---|
| OMD9 | 100/10 | 100/9 (90%)[b] | 78.3 | 8.2 |
| OMD17 | 100/20 | 100/17 (85%) | 70.5 | 9.2 |
| OMD28 | 100/30 | 100/28 (93%) | 89.0 | 10.7 |
| OMD36 | 100/40 | 100/36 (90%) | 89.7 | 11.7 |

[a] Determined by $^1$H-NMR in DMSO-$d_6$ at 20 °C.
[b] Conjugation efficiency calculated as follows: amount of conjugated octadecanol/ amount of octadecanol-CI in feed.
[c] Obtained by theoretical calculation as follows: dextran $M_w$ 70,000 (g/ mol) + number of conjugated octadecanol residues × 301 ($M_w$ of octadecanol residues).
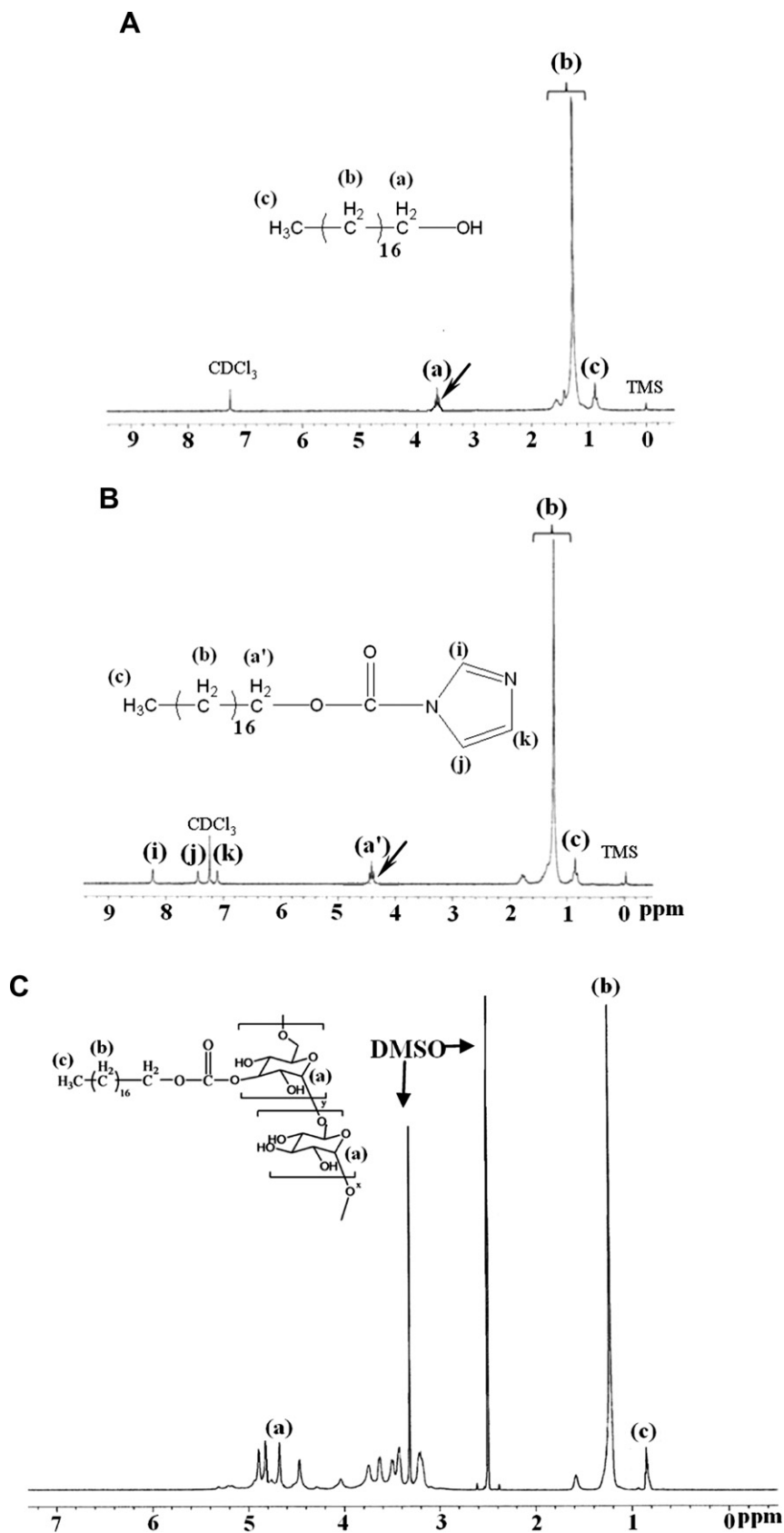
**Fig. 1.** $^1$H-NMR spectra of (A) 1-octadecanol, (B) octadecanol-CI in CDCl$_3$ and (C) OMD17 in DMSO-$d_6$ at 20 °C.

## 2.8. TEM examination

The sample was prepared by placing a few drops of aqueous suspension of OMD assemblies at 25 °C on a 300-mesh copper grid covered with carbon and then allowed to stand for 20 s. Excess solution on the grid was gently removed with absorbent paper. This was followed by negative staining of the sample for 20 s using a uranyl acetate solution (2.0 wt%). The sample was then dried at 25 °C for 2 days. The TEM image was obtained from a JEOL JEM-1200 CXII microscope operating at an accelerating voltage of 120 kV.

## 2.9. LSCM examination

Micro-scaled polysaccharide assemblies in aqueous phase were examined on a Carl Zeiss LSM510 LSCM. The OMD assemblies were stained with either Nile red ($\lambda_{ex}$ = 543 nm, $\lambda_{em}$ = 560—700 nm) (2.0 × 10$^{-10}$ M) as a nonpolar membrane-associated probe alone or FITC-dextran (4 K or 10 K, $\lambda_{ex}$ = 488 nm, $\lambda_{em}$ = 500—600 nm) as a water-soluble fluorescence probes. FITC-dextran was dissolved in the aqueous solution of NaCl (0.01 M) acting as the $w_1$ phase in the double emulsion procedure, as aforementioned in the section of Preparation of Micro-Scaled Polysaccharide Vesicles. The un-encapsulated FITC-dextran in the aqueous vesicle suspension was fully removed by ultrafiltration (Amicon 8200 with a Millipore PBMK membrane, MWCO 300,000) against DI water.

## 3. Results and discussion

### 3.1. Synthesis and characterization of OMD

Compared with the $^1$H-NMR spectrum of 1-octadecanol in CDCl$_3$ at 20 °C (Fig. 1A), the appearance of feature proton signals of imidazole group of 1-octadecanol-CI at $\delta$ 7.1, 7.4 and 8.2 ppm and a complete downfield shift of the $\alpha$-proton signal of the activated octadecanol from $\delta$ 3.6 to 4.4 ppm in the NMR spectrum (Fig. 1B) strongly confirm the successful activation of 1-octadecanol with CDI. Judging from the integration ratio of the characteristic proton signals of octadecanol-CI at $\delta$ 4.4 and 8.2 ppm (Fig. 1B), essentially full activation of 1-octadecanol as depicted in Scheme 1 was attained. The OMD adducts were subsequently obtained by coupling reaction of dextran with 1-octadecanol-CI via carbonate linkage (Scheme 1). Fig. 1C representatively illustrates the $^1$H-NMR spectrum of OMD17 (5.0 mg/mL) in DMSO-$d_6$. Based on the
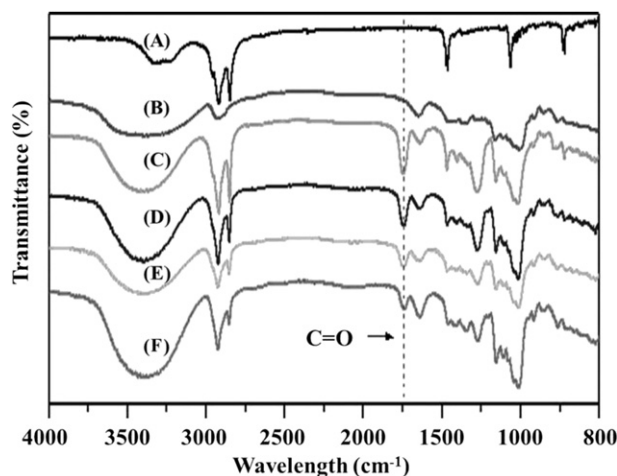
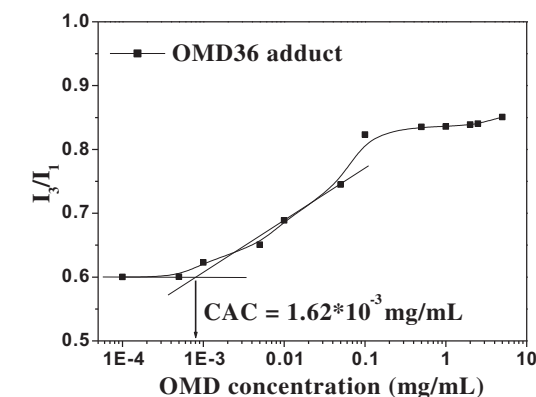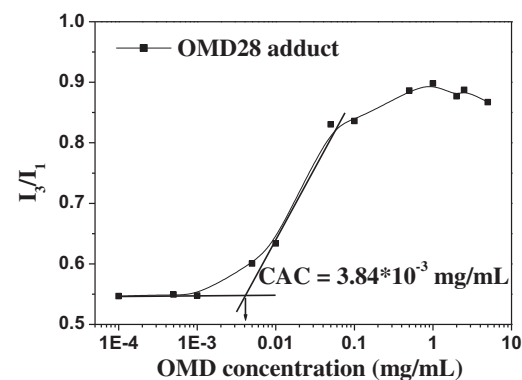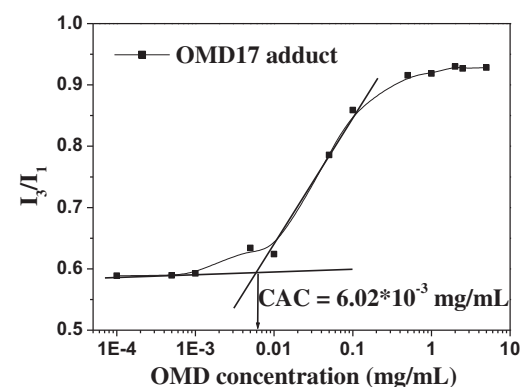**Fig. 2.** FT-IR spectra of (A) 1-octadecanol, (B) dextran, (C) OMD36, (D) OMD28, (E) OMD17, and (F) OMD9.
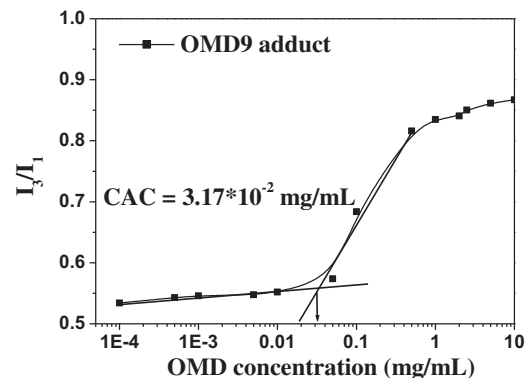
**Fig. 3.** Fluorescence intensity ratio ($I_3/I_1$) of pyrene in aqueous solutions of OMD with DS 9, 17, 28 and 36 as a function of the OMD concentration.

integration ratio of the feature signal from the tail methyl protons of octadecanol residues at $\delta$ 0.82 ppm and that from the anomeric protons of dextran at $\delta$ 4.7 ppm, the conjugation extents in terms of DS were determined, and the results summarized in Table 1. The fact that the conjugation efficiencies, defined as the ratio of the amount of octadecanol residues to that of octadecanol-CI in the reaction feed, are greater than 85% suggests that the DS of OMD can be well controlled simply by adjusting the molar ratio of dextran to octadecanol-CI in the reaction feed. In agreement with the $^1$H-NMR data, the FT-IR spectra (Fig. 2) also show the feature bands at 1743 and 1645 cm$^{-1}$ ascribed to the C=O stretching vibration of carbonate ester linkages and C–H bending vibration of aliphatic alkyl chains of OMD, respectively. In addition, the band intensities are proportional to the DS of these OMD derivatives. The yields of four OMD adducts produced via the current approach are all greater than 70%.

Conjugation of water-soluble dextran with hydrophobic n-octadecyl chain segments cooperatively renders the resulting lipid-modified polysaccharides highly amphiphilic and capable of undergoing assembly via extensive hydrophobic association of lipid chain segments into polymeric colloids in aqueous phase. The CAC values of OMD derivatives in aqueous solutions were evaluated from the fluorescence characterization of pyrene as a nonpolar probe in aqueous solutions of OMD with different concentrations. For every OMD sample, intermolecular assembly occurs at an onset

concentration, defined herein as the CAC, in correspondence to the commencement of a dramatic increase in the $I_3/I_1$ ratio of pyrene (Fig. 3). This is caused by an abrupt increase in microenvironmental hydrophobicity of the probe upon formation of polymeric assemblies comprising nonpolar lipid regions, in which pyrene molecules prefer to reside. Among the four OMD derivatives investigated in this work, OMD36 displays the lowest CAC value ($1.62 \times 10^{-3}$ mg/mL), while OMD9 undergoes self-assembly at a CAC value at least one order of magnitude higher ($3.17 \times 10^{-2}$ mg/mL). The results manifest that the nonpolar nature of OMD derivatives increases significantly with increasing lipid content, thereby facilitating the hydrophobically driven self-association of the OMD derivative containing a higher level of lipid at a lower OMD concentration. Similar results were reported elsewhere [18,37]. More importantly, the morphology of polymeric assemblies depends appreciably on the nonpolar content of OMD adducts and assembling processes adopted. Thus, the versatile OMD polymer assemblies prepared in this work exhibit varying architectures along with unique morphologic characteristics, as described below.

### 3.2. Characterization of nano-scaled OMD vesicles

Fig. 4A illustrates that, when the initial water content of the OMD17 solution in DMSO/H$_2$O is increased to a critical point (e.g., in this case 12.5% (v/v) of the total solution volume) defined hereinafter as the critical water content (CWC) [38–40], supramolecular association of the OMD17 adduct into stable nano-scaled polymeric assemblies with a mono-modal size distribution occurs. It is noteworthy that, with the initial added water content above the CWC, OMD17 assemblies of varying sizes can be thus attained. The DLS
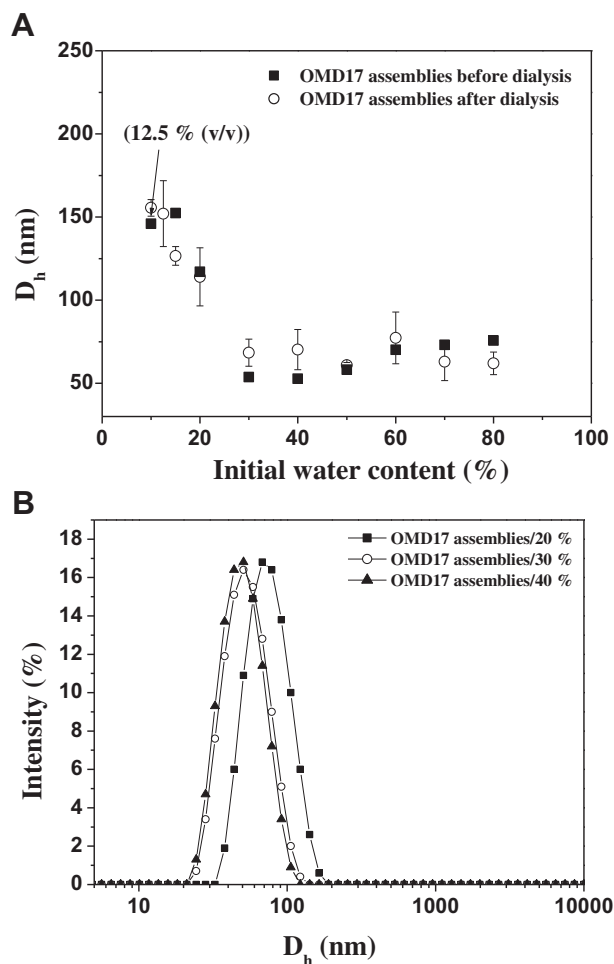


**Fig. 4.** (A) Mean $D_h$ of OMD17 assemblies in DMSO/H$_2$O solutions with different initial water contents before and after removal of DMSO by dialysis. (B) Particle size distribution profiles of OMD17 assemblies developed in DMSO/H$_2$O solutions with different initial water contents prior to dialysis.
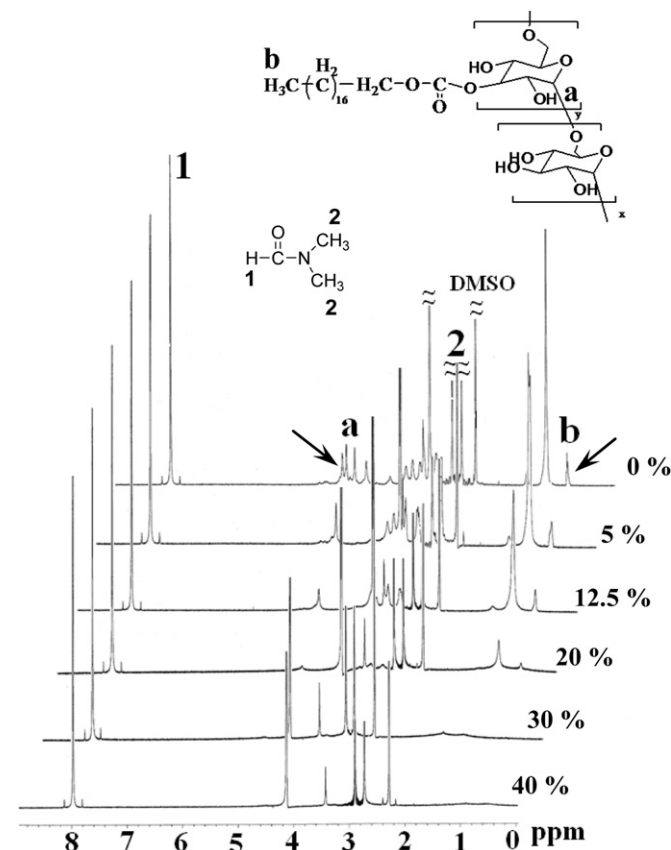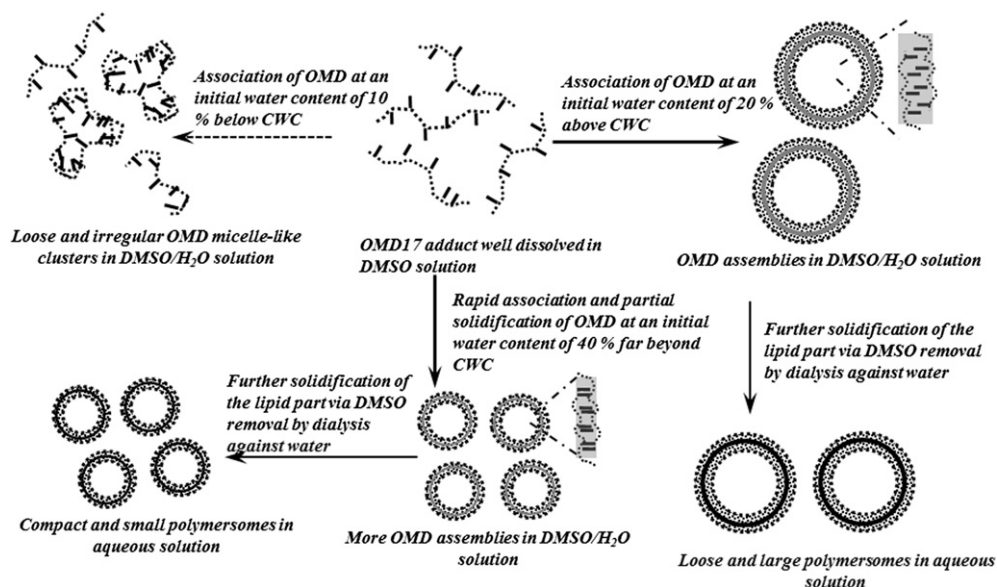


**Fig. 5.** $^1$H-NMR spectra of OMD17 in DMSO-$d_6$/D$_2$O solutions with varying initial D$_2$O contents using DMF in a sealed capillary as an external standard.

**Scheme 2.** Illustration of formation mechanism and characteristics of nano-scaled polymersomes from OMD adducts.

data in Fig. 4A reveal that the aqueous OMD17 colloids after full removal of DMSO by dialysis against DI water still retain essentially identical particle size as compared to their counterparts without the dialysis treatment. Similar results were also observed for the OMD28 assemblies (Fig. S1). Compared to OMD17, OMD28 has a significantly lower CWC (ca 2.5% (v/v)). This is primarily attributed to the fact that the OMD28 adduct comprising more lipid residues shows a strong tendency to associate into stable polymeric assemblies in response to the addition of a rather limited amount of water into the OMD28 solution in DMSO. It becomes apparent that the initial water content of the OMD solution in DMSO/H$_2$O beyond the CWC plays a vital role in determining the assembly process and the resultant colloidal morphology, regardless of the presence of DMSO in the final colloidal products or not. Further studies on the formation mechanism of supramolecular assembly and the effects of the initial water content on the assembly morphology were performed by $^1$H-NMR and DLS/SLS measurements, respectively. As shown in the $^1$H-NMR spectra (Fig. 5), fully detectable characteristic proton signals of octadecanol and dextran parts originating from OMD17 in DMSO-$d_6$ strongly indicate that the OMD adduct is well dissolved. Accompanied with the addition of D$_2$O below CWC (12.5% (v/v)), slight reductions in both signal intensities of anomeric protons from dextran and tail-end methyl protons from octadecanol residues signify the occurrence of hydrophobically driven assembly. Considering the highly nonpolar nature of octadecanol moieties in fully miscible DMSO/H$_2$O solution containing only a small fraction of water, partial amphiphilic OMD17 species undergo hydrophobically driven association most likely into a rather loose irregular micelle-like structure, while the remaining OMD17 species are dissolved in the continuous phase, as depicted in Scheme 2. DLS measurements confirm the very weak light scattering intensity along with the quite broad particle size distribution (PDI 0.64) for the OMD17 assemblies in DMSO/H$_2$O solutions with the initial water contents below the CWC value. This is in qualitative agreement with the above postulated polymeric assembly structure (data not shown here).

For the experiments with the amount of H$_2$O (i.e., D$_2$O in $^1$H-NMR measurements) greater than the CWC, the proton signal intensities of octadecanol residues of OMD17 are reduced correspondingly. This is because the higher the initial water content within the miscible DMSO/H$_2$O solution, the more pronounced the hydrophobic association and the subsequent solidification of

octadecanol residues of OMD, thereby leading to supramolecular assembly. Under the circumstance, appreciable reductions in the alkyl segmental mobility and the corresponding proton signals in the $^1$H-NMR spectra occurred. On the other hand, as illustrated by the DLS data in Fig. 4A, the OMD17 assembly size is greatly reduced from 150 to 40 nm when the initial water content increases from 12.5 to 40% (v/v). This is primarily due to an increase in the number density of colloidal particles along with a decrease in the aggregation number of OMD species within individual assemblies. This is further corroborated by the results obtained from the different-angle DLS/SLS measurements, as shown below.

In Table 2, the $R_g/R_h$ values of OMD17 assemblies developed at the initial water contents of 10, 20 and 40% (v/v) in DMSO/H$_2$O solution are ca 1.56, 1.16 and 0.95, respectively, after thorough removal of DMSO by dialysis. The $R_g$ value of OMD17 assemblies in aqueous phase determined herein by the Berry treatment (Fig. S2) is intimately associated with the mean distance of individual atoms (groups) that constitute the assembly of target to its mass center, while $R_h$ is the radius of a theoretical hard sphere that diffuses with the identical speed to the target colloidal assembly under examination [34]. The $R_g/R_h$ ratio is very susceptible to changes in the assembly topology and thus useful for the structural justification [41,42]. It is generally recognized that a theoretical value of unity represents the typical assembly of dense and thin-layer hollow spheres [41,42]. The $R_g/R_h$ value (1.56) of OMD17 assemblies

**Table 2**

DLS and SLS data of OMD17 polymeric assemblies developed in DMSO/H$_2$O solutions with different water contents after removal of DMSO.

| Sample | Initial water content (% (v/v)) | $R_g$ (nm) | $R_h$ (nm)[a] | $R_g/R_h$ | $M_w/10^8$ (g/mol) | $N_{agg}$[b] |
|--------|------|------|------|------|------|------|
| OMD17 | 10 | 151.1 | 96.0 | 1.56 | 16.5 | 17,930 |
| | 20 | 46.8 | 40.4 | 1.16 | 4.55 | 4940 |
| | 40 | 29.8 | 31.3 | 0.95 | 0.23 | 250 |

[a] Determined by DLS (Brookhaven BI-200SM) at a scattering angle of 90°, using the CONTIN analysis method.
[b] Average number of aggregated OMD species in every polymer-assembled particle obtained by theoretical calculation as follows: (weight-average molecular weight of polymeric assemblies)/(average molecular weight of OMD17 adduct as shown in Table 1).

developed at an initial water content of 10% (v/v) that is below the CWC is representative of the highly loose and irregular structure [41,42], irrespective of the presence or absence of DMSO. By contrast, with the initial water content being increased from 10 to 20 and 40% (v/v), the $R_g/R_h$ values of OMD17 assemblies are reduced from 1.56 to 1.16 and 0.95, respectively. These data strongly indicate the assembly structure in polymersome morphology. Furthermore, structural transformation from relatively loose (in packing density) and large (in size) to compact and small architecture occurs when the initial water content is increased from 20 to 40%. Table 2 also shows the effects of the initial water content on the weight-average molecular weight ($M_w$) and aggregation number of OMD species per colloidal particle ($N_{agg}$), which are in agreement with the

particle size ($R_h$) data estimated by DLS. Apparently, intermolecular packing of lipid/polysaccharide adducts into the vesicle structure is largely governed by the nonpolar content [17,18,43]. The stiffness of polysaccharide backbone chains along with the great tendency of lipid residues with the pertinent alkyl chain length, while experiencing significant hydrophobic association, to accommodate into relatively regular and order bilayer (or interdigitated) configuration may cooperatively promote vesicle formation.

TEM images of OMD17 assemblies developed at an initial water content (40% (v/v)) > CWC in DMSO/H$_2$O solution before (Fig. 6) and after DMSO removal (Fig. S3) further demonstrate the assembly morphology in a hollow spherical structure, as evidenced by the appearance of the clear contrast between the centers and the negatively stained shells with uranyl acetate. The particle size of these OMD-based colloids is inversely proportional to the initial water content up to 30%, in good agreement with the DLS/SLS data (Fig. 4A and Table 2). It should be noted that the particle size observed by TEM is significantly larger than that determined by DLS. This is in part due to the removal of water molecules from the interior of OMD vesicles during the preparation of TEM samples, thereby allowing the dried hollow particles to become flattened and spread on the TEM copper grids. In addition, such a dramatic change of the polymeric assemblies from an aqueous to a low-pressure air environment also inevitably induce appreciable size enlargement. Similar observations were reported in the literature [44,45].

### 3.3. Characterization of micro-scaled OMD vesicles

In addition to the nano-scaled polymersomes discussed above, the micro-scaled counterpart was produced by a double emulsion technique in a w$_1$/o/w$_2$ manner. The OMD36 adduct was chosen for this study, taking advantage of its high octadecanol content in favor of developing stable micro-scaled polymersomes. During the double emulsion formation process, the aqueous NaCl solutions of varying concentrations were used as the inner (w$_1$) phase, and DI water as the continuous aqueous phase (w$_2$), respectively. The co-solvent system of DMSO/CHCl$_3$ (50% (v/v)), in which OMD36 was dissolved, served as the organic phase. The LSCM images (Fig. 7A and B) show the solid-core micelle-like assemblies formed when either DI water or the aqueous NaCl solution of 0.005 M was employed as the w$_1$ phase. Nile red was used as a nonpolar fluorescence probe by associating with the octadecanol-rich regions within colloidal particles for the LSCM examination. By contrast, when 0.01 or 0.1 N NaCl solution was adopted as the w$_1$ phase, spherical polymersomes with the diameters in the range 10–25 μm obviously developed (Fig. 7C and D). These results are primarily attributed to the scenario that, with the NaCl concentration in the w$_1$ phase being raised, the increased ionic osmotic pressure established between the w$_1$ and w$_2$ phase greatly promotes water influx through the intermediate OMD-rich regions into the enclosed aqueous chambers. As a result, DMSO/CHCl$_3$ organic solvents were removed rapidly from OMD-rich regions. This will then promptly facilitate the solidification of the lipid residues of OMD adduct and subsequent formation of micro-scaled polymersomes. The proposed formation mechanism and characteristics of micro-scaled polymersomes from OMD adducts are illustrated in Scheme 3.

On the other hand, when the aqueous solution of NaCl at 0.01 M was selected as the w$_1$ phase and DI water as the w$_2$ phase, the OMD vesicle size can be largely reduced with a gradual increase in the DMSO content of the organic co-solvent in the range 10–80% (v/v), as demonstrated by the LSCM data in Fig. 8. This is primarily because the increase of DMSO, which is much more miscible with water than CHCl$_3$ within the organic phase, results in a reduction in the oil–water interfacial tension (i.e., the total oil–water interfacial free energy) of OMD-containing emulsions in
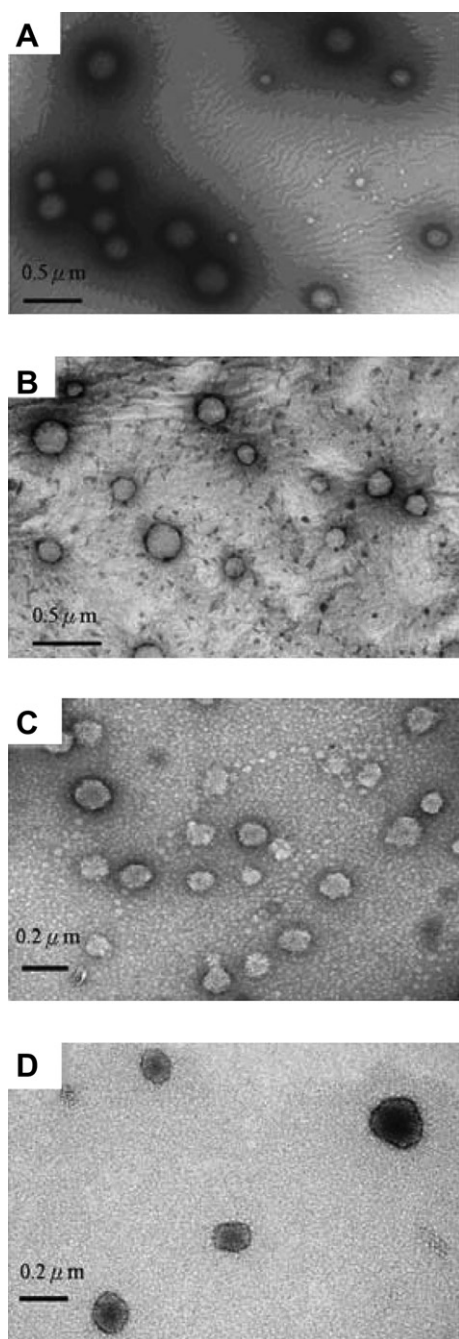


**Fig. 6.** TEM images of OMD17 polymersomes developed in DMSO/H$_2$O solutions with initial water contents of (A) 12.5, (B) 15, (C) 30 and (D) 40% (v/v).
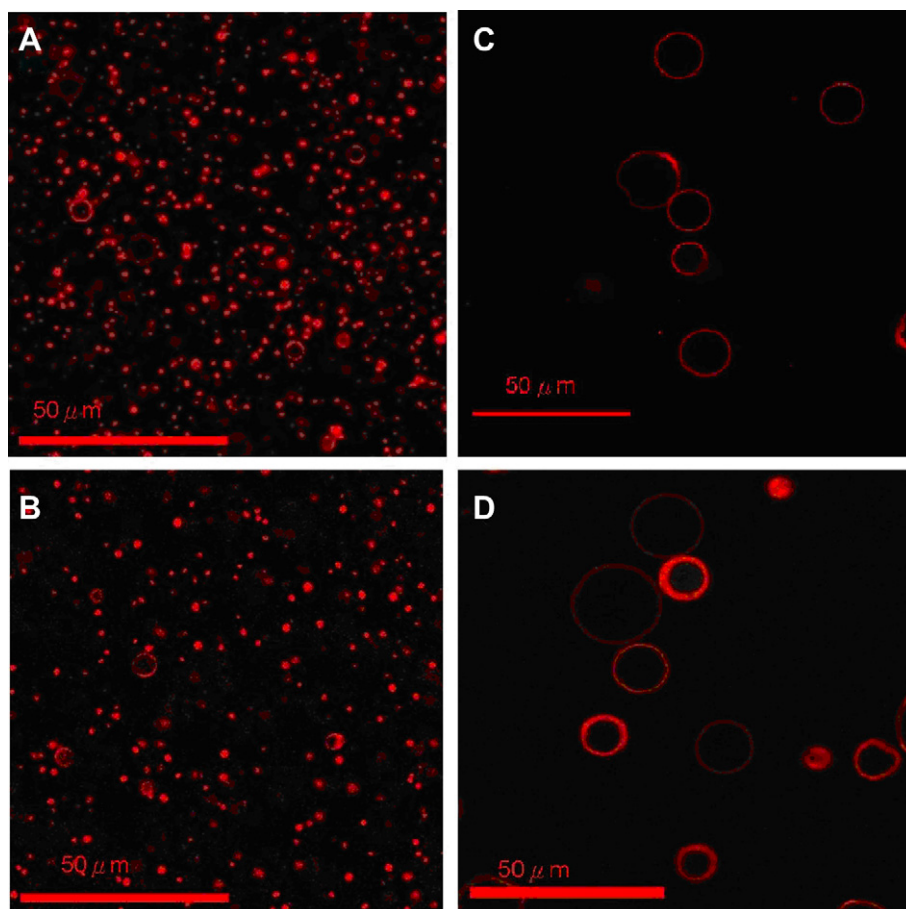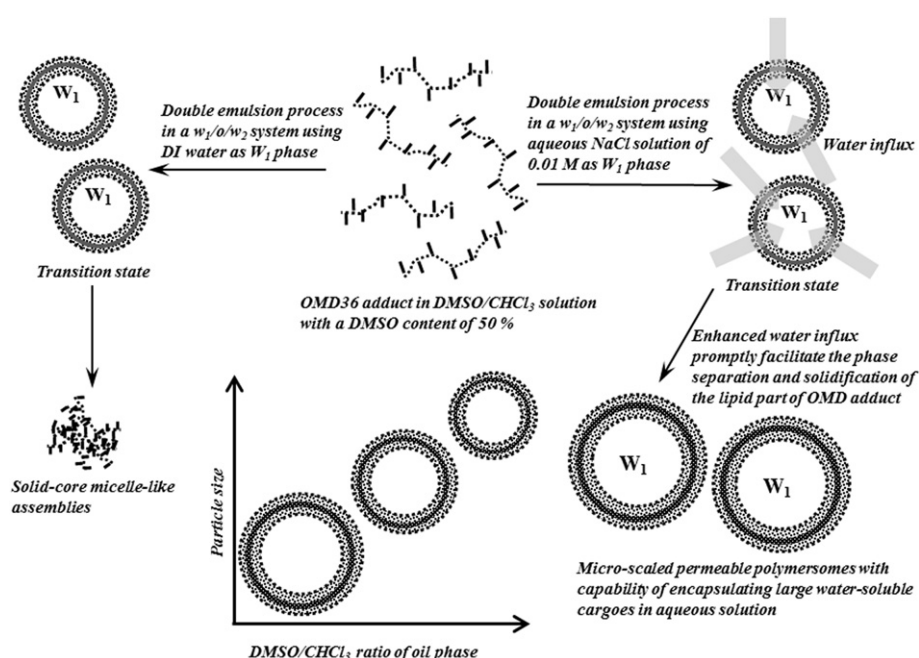
**Fig. 7.** LSCM images of Nile red-stained OMD36 assemblies in aqueous milieu prepared by the double emulsion technique in a $w_1$/o/$w_2$ manner using (A) DI water and aqueous NaCl solutions of (B) 0.005, (C) 0.01 and (D) 0.1 M as the $w_1$ phase, respectively. The co-solvent system of DMSO/CHCl$_3$ with a DMSO content of 50% (v/v) was used as the organic phase, and DI water as the continuous aqueous phase ($w_2$).



**Scheme 3.** Illustration of formation mechanism and characteristics of micro-scaled polymersomes from OMD adducts.
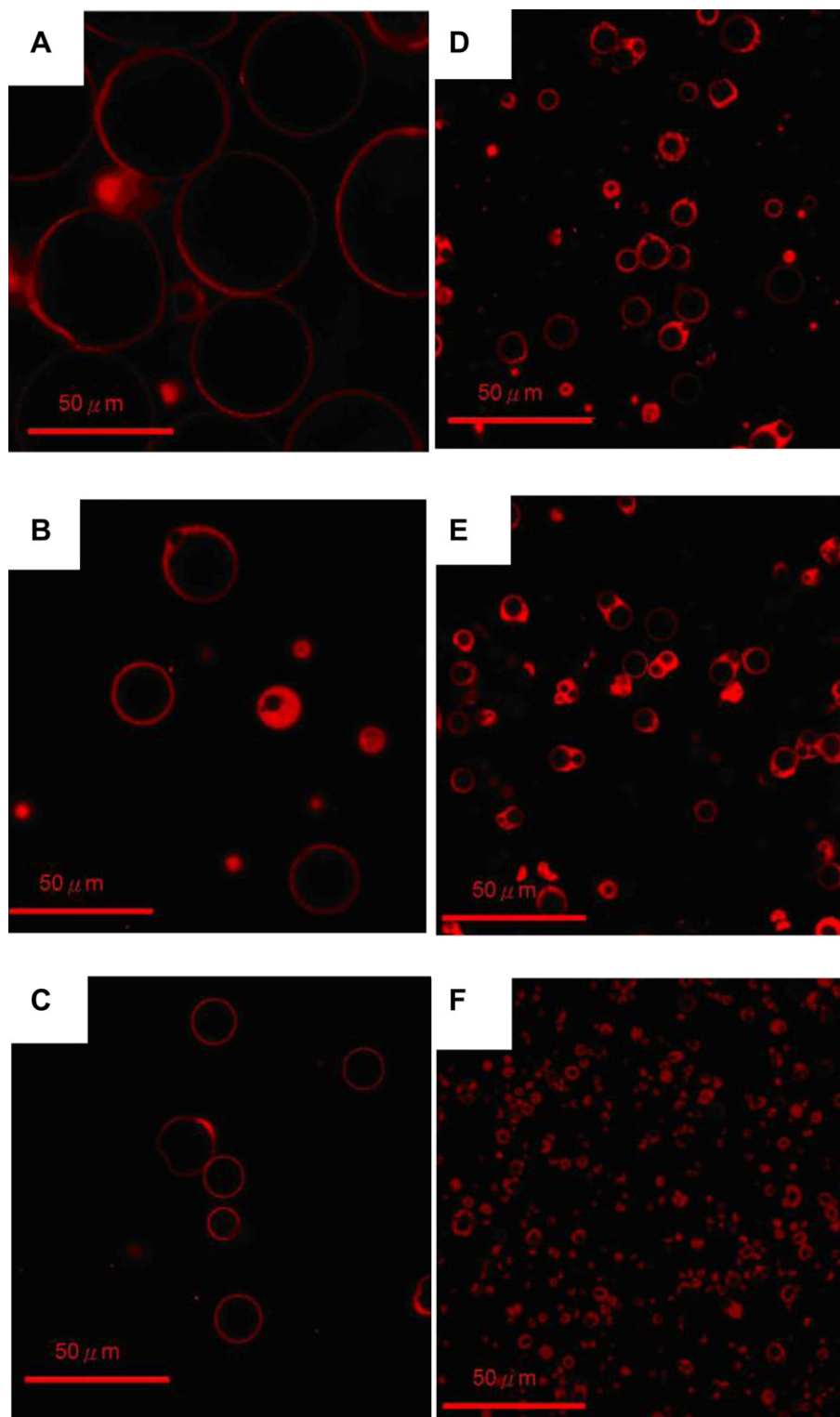
**Fig. 8.** LSCM images of Nile red-stained OMD36 vesicles in aqueous solutions attained by the double emulsion technique using the co-solvent system of DMSO/CHCl$_3$ with the DMSO contents of (A) 10, (B) 20, (C) 50, (D) 60, (E) 70 and (F) 80% (v/v) as the organic phase, and the NaCl aqueous solution of 0.01 M and DI water as the w$_1$ and w$_2$ phases, respectively.

aqueous milieu. Thus, this thermodynamically favorable condition effectively prohibits subsequent particle aggregation and greatly enhances the stability of the colloidal particles of smaller sizes. As a consequence, the morphology and size of OMD assemblies can be easily regulated by both the contents of NaCl in the w$_1$ phase and of DMSO in the organic phase.

To further evaluate the feasibility of using these OMD polymersomes as microcontainers for hydrophilic cargoes, the aqueous solutions of FITC-dextrans 4 K and 10 K were employed, respectively, as the w$_1$ phase. The co-solvent system of DMSO/CHCl$_3$ (50/50 (v/v)) was used as the organic phase. The LSCM images (Fig. 9 and Fig. S4) show that the polar probe fluorescence was seen
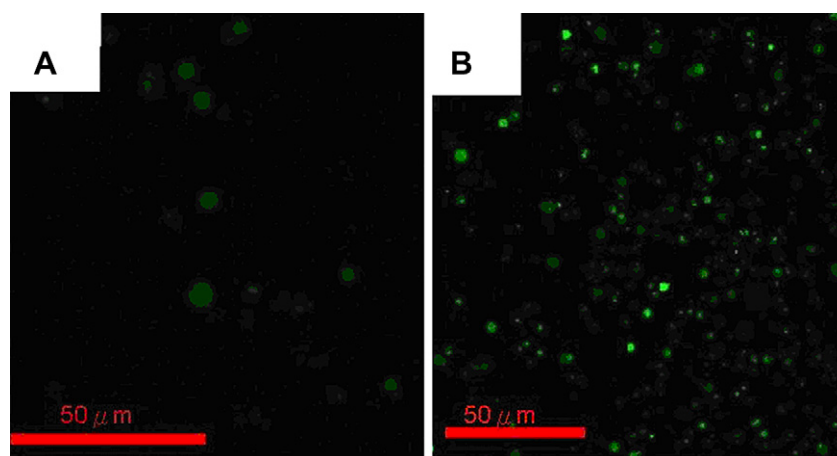
**Fig. 9.** LSCM images of OMD36 polymersomes carrying (A) FITC-dextran 4 K and (B) 10 K in aqueous solutions, respectively.

**Table 3**
Effects of preparation approaches and parameters on the structure of OMD polymersomes.

| Target copolymer/approach | Parameter | Effect |
|---|---|---|
| OMD17, OMD28/partial solvent displacement technique | 1. Lipid content ↑ | 1. CWC of OMD adducts↓ |
| | 2. Initial water content below CWC | 2. Loose and irregular micelle-like clusters |
| | 3. Initial water content above CWC | 3. Loose and large nano-scaled polymersomes |
| | 4. Initial water content far beyond CWC | 4. Compact and small nano-scaled polymersomes |
| OMD36/double emulsion ($w_1/o/w_2$) technique | 1. NaCl concentration in $w_1$ phase below 0.01 M | 1. Solid-core micelle-like assemblies |
| | 2. NaCl concentration in $w_1$ phase above 0.01 M | 2. Micro-scaled permeable polymersomes capable of encapsulating large water-soluble cargoes |
| | 3. DMSO content of the DMSO/CHCl$_3$ co-solvent as the organic phase↑ | 3. Particle size of Macro-scaled permeable polymersomes↓ |

exclusively within vesicular internal aqueous phase, thereby confirming the successful encapsulation of these polar cargoes within polymersomes. Note that the average size (ca. 5 μm) of the vesicles carrying a cargo, either FITC-dextran 10 K or 4 K, is appreciably smaller than that (ca. 20 μm) of the pristine OMD polymersomes. This is most likely due to the interactions between FITC-dextran and dextran segments of OMD adduct that virtually change the $N_{agg}$ value during the assembly formation process. In comparison with FITC-dextrans capable of being confined within polymersomes, another polar fluorescence probe, calcein (MW 622 g/mol), was readily liberated from OMD36 polymersomes and removed by dialysis during the purification process (data not shown here). This strongly indicates that the OMD36 polymersomes are most likely characterized by the wall structure that is permeable to low molecular weight hydrophilic substances. In summary, the OMD polymersomes show the capability of encapsulating large water-soluble cargoes while permeation of small species across vesicular membranes is allowed. The vesicular membranes with size-selective permeability render polymersomes developed herein particularly useful in biomedical technologies such as bio-catalysis where the confinement of biomacromolecules within vesicles is required for retaining active interactions with small molecules only, yet effectively excluding contacts with other approaching biomacromolecules. In this study, the approaches and parameters adopted to prepare OMD polymersomes in both nano- and micro-size and the resulting structural effects are summarized in Table 3.

## 4. Conclusion

OMD conjugates of varying DS values were synthesized by partial esterification of dextran with octadecanol-CI in a well regulated manner. Polymersomes in nano- and micro-size can be readily attained from supramolecular assembly of OMD adducts by the partial solvent displacement and double emulsion technique, respectively. Through the addition of DI water into the OMD solution in DMSO, hydrophobically driven association of OMD adducts into nano-scaled vesicles occurs with the particle size being appreciably influenced by the amount of water added. By contrast, micro-scaled vesicles were successfully prepared by a double emulsion technique in a $w_1/o/w_2$ manner using the DMSO/CHCl$_3$ solution as the organic phase, in which OMD36 was dissolved. With the DMSO fraction in the organic phase being increased, the particle size can be significantly reduced. These micro-scaled OMD vesicles are equipped with size-selective membranes capable of encapsulating large water-soluble cargoes while allowing permeation of small polar species across the membrane.

## Appendix A. Supplementary material

Supplementary data associated with this article can be found, in the online version, at doi:10.1016/j.polymer.2012.03.030.

## References

[1] Yan Q, Yuan J, Cai Z, Xin Y, Kang Y, Yin Y. J Am Chem Soc 2010;132(27): 9268–70.
[2] Discher DE, Eisenberg A. Science 2002;297(5583):967–73.
[3] Rijcken CJF, Soga O, Hennink WE, von Nostrum CF. J Control Release 2007; 120(3):131–48.
[4] Chen W, Meng F, Cheng R, Zhong Z. J Control Release 2010;142(1):40–6.
[5] Borchert U, Lipprandt U, Bilang M, Kimpfler A, Rank A, Peschka-Suss R, et al. Langmuir 2006;22(13):5843–7.

[6] Holowka EP, Sun VZ, Kamei DT, Deming TJ. Nat Mater 2007;6(1):52–7.
[7] Huang YF, Chiang WH, Tsai PL, Chern CS, Chiu HC. Chem Commun 2011; 47(39):10978–80.
[8] Zhang Y, Wu F, Yuan W, Jin T. J Control Release 2010;147(3):413–9.
[9] Chiu HC, Lin YW, Huang YF, Chuang CK, Chern CS. Angew Chem Int Ed 2008; 47(10):1875–8.
[10] Choi HJ, Montemagno CD. Nano Lett 2005;5(12):2538–42.
[11] Rodriguez-Hernandez J, Lecommandoux S. J Am Chem Soc 2005;127(7): 2026–7.
[12] Du JZ, Tang YP, Lewis AL, Armes SP. J Am Chem Soc 2005;127(51):17982–3.
[13] Lomas H, Canton I, MacNeil S, Du J, Armes SP, Ryan AJ, et al. Adv Mater 2007; 19(23):4238–43.
[14] Rameez S, Alosta H, Palmer AF. Bioconjug Chem 2008;19(5):1025–32.
[15] Meng F, Zhong Z, Feijen J. Biomacromolecules 2009;10(2):197–209.
[16] Huang WC, Chiang WH, Lin SJ, Lan YJ, Chen HL, Chern CS, et al. Adv Funct Mater; 2012. doi:10.1002/adfm.201103117.
[17] Besheer A, Hause G, Kressler J, Mader K. Biomacromolecules 2007;8(2): 359–67.
[18] Liu KH, Chen SY, Liu DM, Liu TY. Macromolecules 2008;41(17):6511–6.
[19] Zhang YL, Dou XW, Jin T. eXPRESS Polym Lett 2010;4(10):599–610.
[20] Monchaux E, Vermette P. Langmuir 2007;23(6):3290–7.
[21] Sosa JM. Anal Chem 1980;52(6):910–2.
[22] Hirtenstein M, Clark J, Lindgren G, Vretblad P. Dev Biol Stand 1980;46: 109–16.
[23] Osterberg E, Bergstrom K, Holmberg K, Schuman TP, Riggs JA, Burns NL, et al. J Biomed Mater Res 1995;29(6):741–7.
[24] Schatz C, Louguet S, Le Meins JF, Lecommandoux S. Angew Chem Int Ed 2009; 48(14):2572–5.
[25] Houga C, Giermanska J, Lecommandoux S, Borsali R, Taton D, Gnanou Y, et al. Biomacromolecules 2009;10(1):32–40.
[26] Li YL, Zhu L, Liu Z, Cheng R, Meng F, Cui JH, et al. Angew Chem Int Ed 2009; 48(52):9914–8.
[27] Chiu HC, Lin YF, Hung SH. Macromolecules 2002;35(13):5235–42.
[28] van Dijk-Wolthuis WNE, Tsang SKY, Kettenes-van den Bosch JJ, Hennink WE. Polymer 1997;38(25):6235–42.
[29] Hu XL, Liu S, Chen XS, Mo GJ, Xie ZG, Jing XB. Biomacromolecules 2008;9(2): 553–60.
[30] Sun H, Guo B, Li X, Cheng R, Meng F, Liu H, et al. Biomacromolecules 2010; 11(4):848–54.
[31] Chiang WH, Hsu YH, Tang FF, Chern CS, Chiu HC. Polymer 2010;51(26): 6248–57.
[32] Chiang WH, Hsu YH, Lou TW, Chern CS, Chiu HC. Macromolecules 2009; 42(10):3611–9.
[33] Chen K, Ballas SK, Hantgan RR, Kim-Shapiro DB. Biophys J 2004;87(6): 4113–21.
[34] Schartl W. Light scattering from polymer solutions and nanoparticle dispersions. Heidelberg, Germany: Springer; 2007. pp. 95–148.
[35] Zhang W, Shi L, An Y, Wu K, Gao L, Liu Z, et al. Macromolecules 2004;37(7): 2924–9.
[36] Sinaga A, Hatton TA, Tam KC. Macromolecules 2007;40(25):9064–73.
[37] Du YZ, Weng Q, Yuan H, Hu FQ. ACS Nano 2010;4(11):6894–902.
[38] Zhang Y, Lin W, Jing R, Huang J. J Phys Chem B 2008;112(51):16455–60.
[39] Zhang LF, Eisenberg A. Polym Adv Technol 1998;9:677–99.
[40] Liu X, Wu J, Kim JS, Esenberg A. Langmuir 2006;22(1):419–24.
[41] Niu AZ, Liaw DJ, Sang HC, Wu C. Macromolecules 2000;33(9):3492–4.
[42] Zhang W, Zhou X, Li H, Fang Y, Zhang G. Macromolecules 2005;38(3):909–14.
[43] Ringsdorf H, Schlarb B, Venzmer J. Angew Chem Int Ed 1988;27:113–58.
[44] Feng Z, Fan G, Wang H, Gao C, Shen J. Macromol Rapid Commun 2009;30(6): 448–52.
[45] Liu X, Basu A. J Am Chem Soc 2009;131(16):5718–9.